Sulfonamide – Bovine Serum Albumin Interactions: Insights from Spectral, electrochemical and Molecular Docking Studies

J. Thulasidhasan[1]*, T.Jeyanthi[2], N. Rajendiran[3] , S. Agiladevi[4], J. Kavitha[5], and J. Vidhya[6] , P. Sangaiya[7]

*[1] Department of Chemistry, V. S. B. Engineering College, Karur-639 111, Tamil Nadu, India.
Email ID: dhasant@gmail.com, ORCID ID - 0000-0001-7781-0632
[2]CMS College of Engineering, Eranapuram, Namakkal-637 003, Tamil Nadu, India.
Email ID: jeychemistry1984@gmail.com
[3]Department of Chemistry, Annamalai University, Annamalai Nagar 608 002, Tamil Nadu, India.
Email: drrajendiran@rediffmail.com
[4]K.S.R. College of Engineering, Tiruchengode - 637 215, Tamil Nadu, India.
Email: agilakarmega@gmail.com
[5]Jai Shriram Engineering College, Avinashipalayam, Tirupur- 638 660, Tamil Nadu, India.
Email: kavithajchem@gmail.com
[6]M.Kumarasamy College of Engineering, Thalavapalayam, Karur-639 113, Tamil Nadu, India.
Email: vidhyajcauveryclg@gmail.com
[7] Department of Physics, V. S. B. Engineering College, Karur-639 111, Tamil Nadu, India
Email: sangaiahbose@gmail.com

ABSTRACT
The interactions of the sulfonamide drugs sulfisoxazole (SFO) and sulfathiazole (STO) with bovine serum albumin (BSA) were investigated using UV–visible, fluorescence, cyclic voltammetry, and molecular docking. Spectroscopic studies confirmed stable drug–biomolecule complex formation through concentration-dependent changes in absorbance and fluorescence intensity, with static quenching indicating ground-state complex formation. Binding and Förster resonance energy transfer (FRET) analyses revealed significantly stronger affinity of both drugs toward BSA. Electrochemical studies showed concentration-dependent changes in anodic peak potential, demonstrating altered redox behavior upon biomolecular binding. Molecular docking supported the experimental results, revealing preferential binding of both drugs within subdomain IIA of BSA through hydrogen-bonding and hydrophobic interactions involving the aniline moiety. These findings demonstrate the preferential and stable binding of SFO and STO with BSA, providing molecular-level insights into their binding mechanism, transport, and pharmacokinetic behavior.

***Keywords*:** Sulfa drugs, BSA, Fluorescence quenching, FRET, Molecular docking.
How to cite this article: Thulasidhasan J, Jeyanthi T, Rajendiran N, Agiladevi S, Kavitha J, Vidhya J, Sangaiya P. Sulfonamide – bovine serum albumin interactions: insights from spectral, electrochemical and molecular docking studies. Int J Drug Deliv Technol. 2026;16(73s): 559-567. DOI: 10.25258/ijddt.16.73s.61
Source of support: Nil.
Conflict of interest: None

INTRODUCTION

Serum albumins (SAs) are the predominant proteins in blood plasma and play a vital role in the transport and distribution of a broad spectrum of endogenous and exogenous ligands, including fatty acids, amino acids, metal ions, and pharmaceutical compounds [1–3]. As the major soluble components of the circulatory system, they contribute significantly to physiological regulation. In particular, serum albumins enhance the apparent solubility of hydrophobic drugs in plasma [4] and function as both carrier and storage proteins for various bioactive molecules [5]. Among them, bovine serum albumin (BSA) is widely used as a model protein owing to its close structural similarity to human serum albumin (HSA) [6], making it highly suitable for investigating drug–protein interactions and understanding drug transport mechanisms.

Spectroscopic techniques are extensively utilized for studying protein–drug interactions due to their sensitivity, rapid response, and experimental convenience [7–10]. UV–visible absorption and fluorescence spectroscopy are especially effective for probing molecular interactions and dynamic behavior in biological systems [4]. Fluorescence quenching, in particular, provides a sensitive and non-invasive approach for examining molecular interactions at low concentrations under near-physiological conditions [10]. In this study, fluorescence quenching is employed to evaluate the binding affinity of selected sulfonamide drugs with BSA. In addition, energy transfer processes and drug-induced

conformational changes in BSA are analyzed to elucidate binding mechanisms, fluorophore accessibility, and interaction characteristics.

Sulfonamides, commonly known as sulfa drugs, are synthetic antimicrobial agents widely used in human and veterinary medicine [11–13]. These compounds are structurally defined by a sulfonamide group linked to heterocyclic rings, typically containing five or six members. Despite their widespread application, concerns persist regarding their low biodegradability and potential adverse effects, including neurological disorders, highlighting the importance of understanding their pharmacokinetic and pharmacodynamic properties [14]. Sulfisoxazole (SFO) and sulfathiazole (STO) are representative sulfonamide drugs (Fig. 1) frequently used in veterinary applications for treating infections in poultry, dairy cattle, and other livestock [15,16]. Recent reports have indicated the presence of residual sulfonamides, particularly STO, in food products, raising concerns about their potential impact on human health [17–19]. Therefore, investigating their interactions with biomacromolecules such as proteins is of considerable importance.

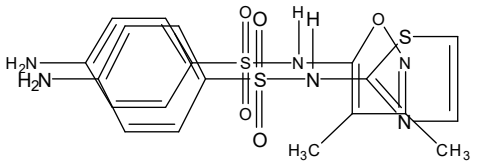

Fig. 1. *Chemical structures of sulfisoxazole (SFO) and sulfathiazole (STO);*

Previous studies on similar systems have primarily focused on elucidating the structural and excited-state properties of organic molecules and their inclusion complexes with cyclodextrins using experimental [20–25] and theoretical approaches [26]. In this context, the present work employs UV–visible & fluorescence spectroscopy, cyclic voltammetry, and molecular docking to systematically investigate the interactions of SFO and STO with BSA. The study focuses on fluorescence quenching mechanisms, determination of binding constants and binding sites, energy transfer efficiency, intermolecular distances, thermodynamic parameters, binding modes, and conformational changes in BSA induced by drug binding.

EXPERIMENTAL SECTION

Materials

SFO, STO, and BSA were obtained from Sigma-Aldrich chemical company and used without further purification. All other reagents were of analytical grade. The purity of the compound was checked by similar fluorescence spectra when excited with different wavelengths. Triply distilled water was used for the preparation of aqueous solutions. BSA solutions were prepared in 2×10^{-5} M Tris HCl buffered at pH 7.4. The concentration of the sulfa drug solutions was varied from 2×10^{-4} to 1×10^{-5} M. 0.2 mL of sulfa drug in methanol solution was used for all binding experiments. All solutions were stored in a refrigerator at 4 °C in the dark.

Instruments

Absorption spectral measurements were carried out with a UV-visible spectrophotometer (model-UV-2600 Shimadzu, Japan) and fluorescence measurements were performed on a spectrofluorophotometer (model-RF-5301PC, Shimadzu, Japan) equipped with 1.0 cm quartz cells. The excitation wavelength for all the sulfa drugs is 280 nm. Cyclic voltammetry measurements were performed through an electrochemical workstation (model-CHI 620D, CH Instruments, USA) with a three electrode system: surface area 0.1963 cm^2 platinum disc as working electrode, saturated silver electrode as reference electrode and a platinum foil as counter electrode. Prior to use, the working electrode was polished with 0.05 μm alumina and thoroughly washed in an ultrasonic bath for 5 min. Before experiments, the solution within a single-compartment cell was deaerated by purging with pure N_2 gas for 5 min. The pH values in the range 2.5-11.5 were measured on Elico pH meter model LI-120.

Molecular Docking

Docking calculations were carried out using Docking Server (http://www.dockingserver.com) [27]. The MMFF94 force field was used for energy minimization of the drug (SFO and STO) molecules using Docking Server [28]. Gasteiger partial charges were added to the drug atoms. Non-polar hydrogen atoms were merged, and rotatable bonds were defined. Docking calculations were carried out on *4F5S* protein model. Essential hydrogen atoms, Kollman united atom type charges, and solvation parameters were added with the aid of Auto Dock tools [29]. Affinity (grid) maps of 20×20×20 Å grid points and 0.375 Å spacing were generated using the Auto grid program [29]. Auto Dock parameter set- and distance-dependent dielectric functions were used in the calculation of the van der Waals and the electrostatic terms, respectively. Each docking experiment was derived from 10 different runs that were set to terminate after a maximum of 25 $x10^4$ energy evaluations. The population size was set to 150. During the search, a translational step of 0.2 Å, and quaternion and torsion steps of 5 were applied.

RESULT AND DISCUSSION

UV spectral studies

Concentration of drugs (M) 10^{-5}	BSA					
	SFO			STO		
	λ_{abs}	log ε	λ_{flu}	λ_{abs}	log ε	λ_{flu}
0 (without drug)	278	4.53	338	278	4.56	338
1	278	4.51	338	278	4.55	338
3	278	4.49	338	277	4.53	338
5	279	4.48	338	277	4.51	339
7	279	4.46	338	277	4.49	339
9	279	4.45	338	277	4.42	339
10	279	4.43	339	277	4.43	340
Excitation wavelength (nm)		-	280		-	280
R_0 (10^{-9})		-	0.7		-	0.8
J (10^{-14})		-	1.8		-	1.9
r (10^{-9})		-	1.0		-	0.9
E			0.42			0.44

Tables 1 present the absorbance and fluorescence spectral data of BSA in the presence of varying concentrations of sulfa drug molecules. In aqueous solution, BSA exhibit characteristic absorption maxima at 278 nm, while the sulfa drugs show an absorption maximum around 262 nm. The observed similarity in the absorption maxima of the sulfa drugs can be attributed to the presence of tautomeric forms within their molecular structures. [30,31] (Fig 2).

Table S1 Absorption and fluorescence maxima of adenine and BSA with different concentrations of SFO and STO.

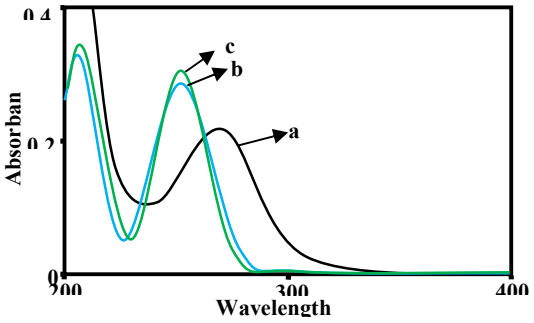

Fig. 2. *Absorbance spectra of (a) BSA, (b) SFO and (c) STO.*

In BSA, a weak absorption peak is observed at 278 nm (Table 1 and Fig. 3), which is attributed to the presence of aromatic amino acid residues such as tryptophan (Trp), tyrosine (Tyr), and phenylalanine (Phe) [32]. It is well established that the absorption characteristics of a chromophore undergo shifts in both wavelength and intensity depending on whether it is located in a hydrophilic or hydrophobic environment. These spectral changes are mainly associated with alterations in the π–π* electronic transitions, resulting from variations in the solvent's polarizability. [33].

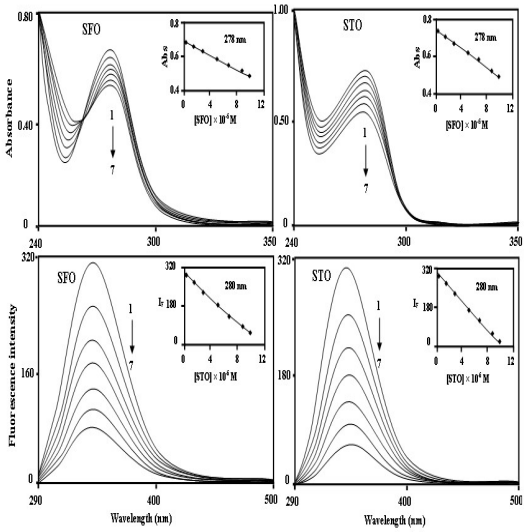

Fig. 3. *Absorbance and fluorescence spectra of BSA with different concentrations of SFO and STO (x 10^{-5} M): 1) 0, 2) 1, 3) 3, 4) 5, 5) 7 and 6) 9 7) 10; Inset fig.: absorbance (Abs) and fluorescence intensity (I_F) vs. [drug].*

Upon the addition of sulfa drug molecules to BSA solutions, the characteristic absorption peak of the drugs disappears, while the absorption maxima of BSA remain unchanged (Fig. 3). A gradual decrease in the absorbance of BSA is observed with increasing drug concentration (insets of Fig. 3), indicating the formation of drug–biomolecule complexes. This reduction in absorbance suggests significant interaction between the sulfa drugs and BSA. These findings further imply that the microenvironment surrounding the chromophoric residues of BSA is altered upon drug binding [34,35]. Additionally, a moderate blue shift in the absorption maxima is observed, suggesting that the peptide chains of BSA adopt a more extended conformation, accompanied by a decrease in hydrophobicity in the local environment.

Fluorescence Spectra

The fluorescence spectra of BSA in aqueous solution at varying concentrations of sulfa drugs are presented in Table 1 and Fig. 3. Significant alterations in the fluorescence behavior of BSA are observed upon the addition of sulfa

drugs. In aqueous medium, the emission maxima of SFO and STO are centered at 340 nm. This similarity arises from the isoelectronic nature of their heterocyclic moieties (oxazole and thiazole rings), leading to comparable electronic transitions. Consequently, the emission observed at 340 nm is primarily attributed to the phenyl ring of the drug molecules [30,31].

The observed emission spectral variations of BSA in the presence of sulfa drugs suggest that the amino groups of the drug molecules participate in interactions with the biomolecular systems, particularly the protein (further supported by molecular docking results). This interpretation is based on the principle that fluorescence quenching encompasses processes that reduce emission intensity, including energy transfer, ground- and excited-state complex formation, and collisional interactions [36]. Sulkowska [37] reported that phenylalanine exhibits a very low quantum yield, while the fluorescence of tyrosine is significantly quenched when ionized or when located near amino, carboxyl, or tryptophan residues. Consequently, the intrinsic fluorescence of BSA is predominantly governed by tryptophan residues. In the present study, the fluorescence intensity of BSA decreases progressively with increasing concentrations of sulfa drugs, whereas the emission maxima and spectral profiles remain essentially unchanged. This behavior indicates that the drug molecules interact with BSA, leading to fluorescence quenching without causing significant alterations in the immediate microenvironment of the tryptophan chromophores.

Fluorescence Quenching Analysis

To elucidate the binding mechanism between BSA and the sulfa drugs, fluorescence quenching studies were carried out using the Stern–Volmer relationship, as represented in Equation (1).

$$F_0/F = 1 + K_{SV}[Q] = 1 + K_q\tau_0[Q] \quad (1)$$

Figure 4 illustrate the Stern–Volmer plots of $[(F_0 - F)/F]$ versus quencher concentration [Q]. A strong linear correlation is observed, indicating that the quenching process follows either a collisional (dynamic) or static mechanism [38–41]. The Stern–Volmer quenching constants (K_{sv}) and bimolecular quenching rate constants (kq) were determined from Eq. (1) at different concentrations of sulfa drugs (Table 2).

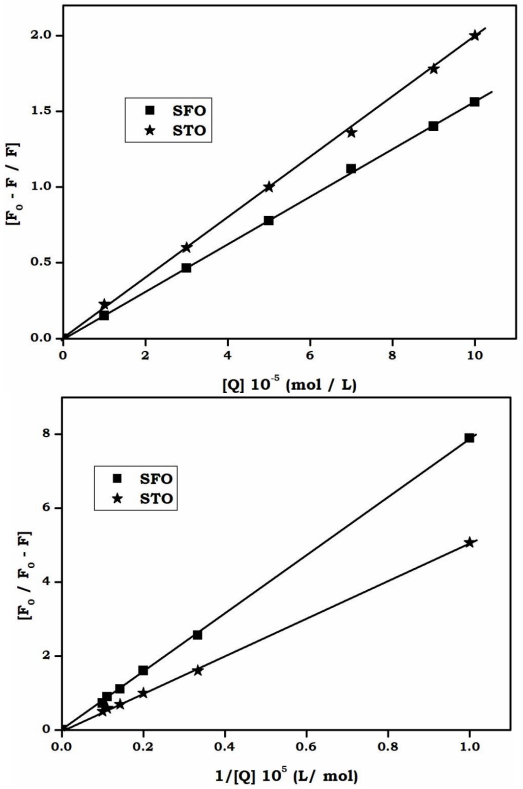

Fig. 4. *Stern-Volmer plots for fluorescence quenching of BSA by SFO and STO at 300 K C_{BSA} = 2.0 × 10^{-5} M; pH 7.4; λ_{ex} = 280 nm, λ_{em} = 290–500 nm*

It is further observed that both Ksv and kq decrease with increasing drug concentration. Notably, the calculated kq values significantly exceed the maximum diffusion-controlled quenching constant (2 × 10^{10} M^{-1} s^{-1}), indicating that the observed fluorescence quenching cannot be attributed to dynamic collisional processes. Instead, the results point toward a static quenching mechanism arising from specific interactions between the sulfa drugs and BSA. Therefore, the quenching behavior was further analyzed using the modified Stern–Volmer equation (Eq. 2).

$$\frac{F_0}{\Delta F} = \frac{1}{f_a K_a}\frac{1}{[Q]} + \frac{1}{f_a} \quad (2)$$

Figures 4 depict the double reciprocal plots of $[F_0/(F_0 - F)]$ versus $[Q]^{-1}$. A strong linear relationship is observed, confirming the applicability of the modified Stern–Volmer equation. The calculated parameters are summarized in Table 2.

Table. 2. *Stern-Volmer quenching constant (Ksv), modified Stern-Volmer association constant (K_a) and bimolecular quenching rate constant (Kq) of adenine and BSA with SFO and STO at 308 K; λ_{ex} = 280 nm, λ_{em} = 290–500 nm, (pH – 7.4)*

	Drugs	**K_{sv}(10^4 M^{-1})**	**K_q(10^{12} $M^{-1}s^1$)**	**R^a**	**SD**
S-V quenching	SFO	1.860	1.86	0.999	0.592
	STO	2.140	2.14	0.999	0.761
Modified S-V quenching	**Drugs**	**K_a (10^4 M^{-1})**	**n**	**ΔG (kJ/mol)**	**R^a**
	SFO	1.379	0.97	-20.93	0.9996
	STO	1.417	0.99	-20.98	0.9986

K_{sv} and K_q - values obtained from eqn (1); n - Number of binding site ***;*** *n - values obtained from eqn (3);* ***R^a-*** *linear correlation coefficient,* ***SD*** *– Standard deviation*

The observed linearity indicates the presence of a single class of accessible fluorophores and validates the formation of a stable complex between the sulfa drugs and BSA. These findings further support that the fluorescence quenching mechanism is predominantly static in nature, arising from the formation of a ground-state drug–BSA complex rather than dynamic collisional interactions [33].

Binding Sites and Binding Constant

The relationship between fluorescence quenching intensity and the concentration of the sulfa drugs can be described by the double logarithm regression Eqn (3) [42,43].

$$\log (F_0 - F) / F = \log K_a + n \log [Q] \quad (3)$$

Fig. 5 shows the plot of log[(F_0–F)/F] vs. log[Q]. A good linear relationship between log[(F_0–F)/F] and log[Q] was noticed.

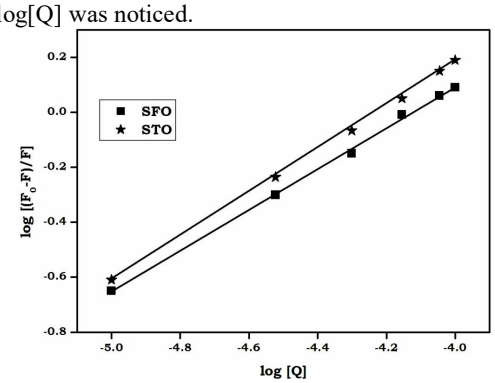

Fig. 5 *Plots of log [(F_0 − F)/F] versus log [Q] for BSA with SFO and STO at 300 K; C_{BSA} = 2.0 × 10^{-5} M; pH 7.4; λ_{ex} = 280 nm, λ_{em} = 290–500 nm*

The results in Table 2, illustrates that there is a strong binding force between sulfa drugs with BSA, and a binding site would be formed. The correlation coefficients are larger than 0.98 indicating that the interaction between sulfa drugs and BSA agrees well with the site binding model underlying Eq. (3).

Free Energy Change and Nature of the Binding Forces

The free energy change (ΔG°) for the binding process was calculated using the following relation (Eq. 4).

$$\Delta G = - \ln K RT \quad (4)$$

Meanwhile, the negative value of ΔG^0 indicated (Table 2) the spontaneity of the binding between sulfa drugs and BSA.

Fluorescence Resonance Energy Transfer (FRET)

FRET is a consistent method for studying protein–drug interactions and estimation of the distance between the drug and protein. The energy transfer efficiency (E) is calculated by the Eq. (5), where r is the distance between the acceptor and the donor, and R_0 is the critical distance, at which 50% of the excitation energy is transported to the acceptor. R_0 can be calculated from donor emission and acceptor absorption spectra using Eq. (6).

$$E = 1 - F / F_0 = R_0 / (R_0^6 + r^6) \quad (5)$$

$$R_0^6 = 8.79 \times 10^{-25} K^2 n^{-4} \varphi J \quad (6)$$

$$J = \frac{\int_0^\infty F(\lambda)\, \varepsilon(\lambda)\, (\lambda)^4\, d\lambda}{\int_0^\infty F(\lambda)\, d\lambda} \quad (7)$$

From Eqs. (5)–(7) [39,40], the Förster resonance energy transfer (FRET) parameters were calculated for the interaction of BSA with SFO and STO drugs. The obtained values are as follows: J = 1.82 and 1.91 × 10^{-14} cm^3 L mol^{-1}, R_0 = 0.78 and 0.82 nm, E = 0.42 and 0.44, and r = 1.01 and 0.98 nm, respectively (Table 1).

The calculated donor–acceptor distances (r) are less than 8 nm and fall within the range of $0.5R_0 < r < 1.5R_0$ [43], satisfying the essential criteria for Förster's non-radiative energy transfer theory. These observations confirm that energy transfer occurs between BSA and the sulfa drugs,

supporting a static quenching mechanism involving ground-state complex formation. Table 1 shows that the energy transfer efficiency (E) for the STO systems is greater than that for SFO. This trend is consistent with the higher Stern–Volmer quenching constants (Ksv) observed for STO with both BSA, further reinforcing the stronger interaction of STO relative to SFO.

ATR - IR spectroscopy

In order to obtain detailed information of BSA conformation after interaction between BSA and the drugs, we have recorded the ATR-IR spectra of the free sulfa drugs, free BSA and BSA with the drugs are shown in Figs. 6. The peak near 1650 cm^{-1} in Fig. 6(a) is the amide I band. It results from the C=O stretching vibrations of the peptide bond. Similarly, the peaks near 1540 cm^{-1} (N-H bending vibration/C-N stretching vibration) and the amide II band, and amide III band, respectively. The peak near 3300 cm^{-1} is thought to be N-H bending vibration and the peak near 1400 cm^{-1} to result from protein side-chain COO^-. As the absorption peak position and shape of the amide I band differ according to the secondary structure, peak analysis can yield information on the secondary structure.

The FTIR spectra of SFO, STO and their interaction with BSA were also studied.

(i) SFO Fig. 6(b): The sharp NH stretch at 3381 cm^{-1} and amido stretch at 3327 cm^{-1} become broad in their BSA interaction. The CH stretch at 3097 cm^{-1} is lost. The C=C stretch at 3006 cm^{-1} does not appear in their BSA complex. The C=C bending at 1579 cm^{-1} shifts to BSA complex at 1449 cm^{-1}. The C–NH_2 stretch at 1303 cm^{-1} is moved to 1393 cm^{-1} in the BSA complex.

(ii) STO Fig. 6(c): The C=N thiazole ring band at 1532 cm^{-1} was shifted to higher frequencies, appearing at 1604 cm^{-1} in the IR of the complex. Further the absorption intensity ratio between the drugs and the interaction with BSA complexes are variable.

Changes in spectral shape and band position of pure drugs, pure BSA and the BSA-drug complexes confirm the formation of the complexes. It was clear that the amide I bands of BSA-drugs system shifted from 1649.2 to 1648 and 1667 cm^{-1} in SFO and STO respectively. Similarly, amide II bands shifted from 1540 cm^{-1} to 1449 and 1448 cm^{-1} in SFO and STO respectively. This indicated the change in secondary structure of BSA upon binding to the drugs.

Cyclic Voltammetry Studies

Upon addition of sulfa drugs to BSA solution, the oxidation and reduction peaks shifted towards high and low potentials respectively. With on the addition of drugs with BSA, a increase on anodic peak current (I_{pa}) with significant shift in peak potential (E_p) was observed. The reason for the increase of the reductive peak current after the reaction of the drugs with BSA, the fallowing factors to be considered:

(*i*) competitive adsorption between the drugs and BSA on the mercury electrode; (*ii*) formation of electrochemical active complex and the changes of electrochemical parameters; (*iii*) formation of electro inactive complex without the changes of electrochemical parameters.

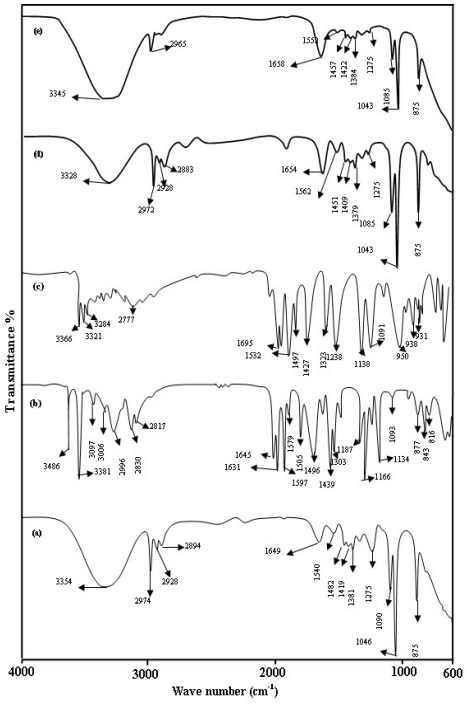

Fig. 6. *FT-IR spectra of FTIR spectra of (a) BSA, (b) SFO, (c) STO (d) BSA - SFO and (e) BSA - STO.*

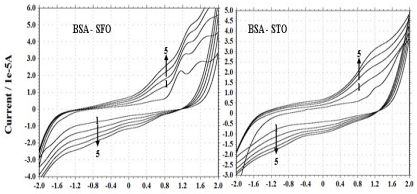

Fig. 7*. Cyclic voltammograms of BSA in presence of SFO and STO with different scan rate (100 to 500 mV s^{-1}). (C_{drugs} = 1 x 10^{-3} M).*

Cyclic voltammograms of sulfa drugs in BSA solution (pH~7.4) and the effect of scan rate on the peak current of the drugs were investigated. From the cyclic voltammograms with scan rate (Fig. 7), it can be seen that the electrode reaction of the drugs in BSA are reversible processes. The peak current was proportional to the root of scan rate over a range of 100 to 1000 mV s^{-1}.

Molecular Docking Studies

The calculated binding free energies (ΔG) for SFO and STO were −7.48 and −7.63 kcal mol⁻¹, respectively. As presented in Table 3, the estimated contributions from van der Waals forces and hydrogen bonding interactions indicate that the BSA–STO complex exhibits a more negative free energy compared to the other systems. This suggests that STO has a stronger binding affinity toward BSA than SFO.

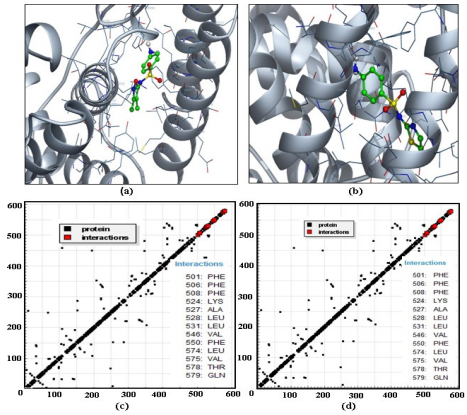

Fig. 8. *The best binding mode between BSA with (a) SFO and (b) STO. The important residues of BSA are represented using lines and the drug structure is represented using a "Ball and Stick" format. Hydrogen bonding plots between BSA with (c) SFO and (d) STO. Colour of the atoms: skeleton structure – BSA, blue- nitrogen, red – oxygen, yellow –sulphur, green- carbon (Fig. 7a and 7b). The BSA residues are represented using black dots and the hydrogen bonding interactions are represented using red dots (Fig. 7c and 7d).*

Molecular docking analysis revealed that all the investigated sulfa drugs preferentially bind within the hydrophobic cavity of subdomain IIA of BSA (Fig. 8). To gain further insight into the binding environment, the amino acid residues surrounding the binding pocket were analyzed. Interaction maps depicting hydrogen bonding and hydrophobic contacts (Fig. 8) highlight the key interactions stabilizing the complexes.

In the BSA–drug systems, the sulfonyl oxygen atoms (O1 and O3) of the sulfa drugs act as hydrogen bond acceptors, forming interactions with ARG458 (–O···H–C, 2.04 Å, 105.7°). For the BSA–SFO complex, an additional hydrogen bond is observed between the nitrogen atom at the N3 position of the drug and the hydroxyl group of LYS524 (–N3···OH, 2.58 Å). In contrast, the BSA–STO complex exhibits hydrogen bonding involving the sulfonyl oxygen (O1) and the aniline nitrogen (N1), interacting with THR578 (–O1···HO, 3.42 Å) and LYS524 (–N1···O, 2.66 Å), respectively.

Moreover, π–cation interactions are observed between the aromatic ring of the sulfa drugs and the –NH_2 groups of PHE501 and PHE550. Additional stabilization arises from hydrophobic contacts with residues such as ALA527, LEU531, and VAL575 located at the periphery of the binding pocket.

Human serum albumin (HSA), which shares significant structural homology with BSA, exhibits a similar binding behavior. Based on the docking results, it can be concluded that hydrophobic interactions, along with hydrogen bonding and other polar contacts, play a dominant role in stabilizing the drug–protein complexes.

CONCLUSION

The interactions of sulfisoxazole (SFO) and sulfathiazole (STO) with bovine serum albumin (BSA) were comprehensively investigated using complementary spectroscopic, electrochemical, and molecular docking approaches. UV–visible absorption and fluorescence measurements confirmed the formation of stable drug–biomolecule complexes, accompanied by significant fluorescence quenching arising from a static quenching mechanism, indicative of ground-state complex formation. Quantitative binding analysis revealed that both sulfonamide drugs possess a markedly higher affinity for BSA, as evidenced by larger binding constants and favorable FRET parameters. Thermodynamic analysis demonstrated that the binding process is spontaneous and primarily governed by hydrogen bonding and van der Waals interactions. Electrochemical studies further supported complex formation by revealing notable changes in the redox behavior of the drugs upon interaction with the biomolecules. Molecular docking corroborated the experimental observations, indicating preferential binding of both SFO and STO within subdomain IIA of BSA through hydrogen-bonding and hydrophobic interactions, with the aniline moiety playing a key role in molecular recognition. Collectively, these findings demonstrate that SFO and STO interact more strongly and stably with BSA, providing molecular-level insights into their binding mechanisms and contributing to a better understanding of their transport, distribution, and pharmacokinetic behavior. The integrated experimental and computational strategy employed in this study also highlights the effectiveness of combining spectroscopic, electrochemical, and docking techniques for elucidating drug–biomolecule interactions.

Funding

The authors declare that no funding was received for this research work.

REFERENCES

1. C. V. Kumar, A. Buranaprapuk, G. J. Opiteck, M. B. Moyer, S. Jockusch and N. Turro, *Proc. Natl. Acad. Sci. U.S.A.*, **95**, 10361–10366 (1998).
2. C. V. Kumar and A. Buranaprapuk, *Angew. Chem. Int. Ed.*, **36**, 2085–2087 (1997).
3. N. Shahabadi, M. Maghsudi and S. Rouhani, *Food Chem.*, **135**, 1836–1841 (2012).
4. Y. J. Hu, Y. Liu, J. B. Wang, X. H. Xiao and S. S. Qu, *J. Pharm. Biomed. Anal.*, **36**, 915–919 (2004).
5. X. L. Han, F. F. Tian, Y. S. Ge, F. L. Jiang, L. Lai, D. W. Li, Q. L. Yu, J. Wang, C. Lin and Y. Liu, *J. Photochem. Photobiol. B*, **109**, 1–11 (2012).
6. S. Nafisi, G. B. Sadeghi and A. PanahYab, *J. Photochem. Photobiol. B*, **105**, 198–202 (2011).
7. P. Abassi, F. Abassi, F. Yari, M. Hashemi and S. Nafisi, *J. Photochem. Photobiol. B*, **122**, 61–67 (2013).
8. T. Sadigh Vishkaee, N. Mohajerani and S. Nafisi, *J. Photochem. Photobiol. B*, **119**, 65–70 (2013).
9. P. N. Naik, S. A. Chimatadar and S. T. Nandibewoor, *Spectrochim. Acta A*, **73**, 841–845 (2009).
10. N. Barbero, E. Barni, C. Barolo, P. Quagliotto, G. Viscardi, L. Napione, S. Pavan and F. Bussolino, *Dyes Pigments*, **80**, 307–313 (2009).
11. X. J. Guo, L. Zhang, X. D. Sun, X. W. Han, C. Guo and P. L. Kang, *J. Mol. Struct.*, **928**, 114–120 (2009).
12. C. C. Brackett, H. Singh and J. H. Block, *Pharmacotherapy*, **24**, 856–870 (2004).
13. C. T. Supuran, A. Casini and A. Scozzafava, *Med. Res. Rev.*, **23**, 535–558 (2003).
14. T. Trenque, G. Hoizey and D. Lamiable, *Diabetes Care*, **24**, 792–793 (2001).
15. D. M. Davies, *Textbook of Adverse Drug Reactions*, Oxford University Press, New York (1985).
16. J. F. Prescott, B. J. Desmond and R. D. Walker, *Antimicrobial Therapy in Veterinary Medicine*, Iowa State University Press (2000).
17. V. Jimenez, J. Adrian, M. P. Guiteras, M. P. Marco and R. Companyo, *J. Agric. Food Chem.*, **58**, 7526–7531 (2010).
18. A. L. Boreen, W. A. Arnold and K. McNeill, *Environ. Sci. Technol.*, **38**, 3933–3940 (2004).
19. I. S. Nesterenko, M. A. Noke and S. A. Eremin, *J. Anal. Chem.*, **64**, 435–444 (2009).
20. A. A. M. Prabhu, G. Venkatesh and N. Rajendiran, *J. Soln Chem.*, **39**, 1061–1086 (2010).
21. J. P. Kumari, A. A. M. Prabhu, G. Venkatesh, V. K. Subramanian and N. Rajendiran, *Phys. Chem. Liq.*, **49**, 108–132 (2011).
22. N. Rajendiran, G. Venkatesh and T. Mohandoss, *Spectrochim. Acta A*, **123**, 158–166 (2014).
23. N. Rajendiran, T. Mohandoss and G. Venkatesh, *Spectrochim. Acta A*, **124**, 441–450 (2014).
24. N. Rajendiran, G. Venkatesh and J. Saravanan, *Spectrochim. Acta A*, **129**, 157–162 (2014).
25. N. Rajendiran and S. Siva, *Carbohydr. Polym.*, **101**, 828–836 (2014).
26. G. Venkatesh, T. Sivasankar and N. Rajendiran, *J. Incl. Phenom. Macrocycl. Chem.*, **77**, 309–318 (2013).
27. Z. Bikadi and E. Hazai, *J. Cheminform.*, **1**, 1–5 (2009).
28. T. A. Halgren, *J. Comput. Chem.*, **17**, 490–519 (1996).
29. G. M. Morris and D. S. Goodsell, *J. Comput. Chem.*, **19**, 1639–1662 (1998).
30. M. G. Wen, X. B. Zhang, J. N. Tian, S. H. Ni, H. D. Bian and Y. L. Huang, *J. Soln Chem.*, **38**, 391 (2009).
31. X. Guo, K. Jing, C. Guo, Y. Jiang, J. Tong and X. Han, *J. Lumin.*, **130**, 2281 (2010).
32. M. Y. Meirong, Z. S. Zhishan, F. J. Fusheng, X. D. Xinghong, J. S. Jinyue and C. S. Suhong, *Spectrochim. Acta A*, **83**, 453 (2011).
33. M. Bhattacharyya, U. Chaudhuri and R. K. Poddar, *Biochem. Biophys. Res. Commun.*, **167**, 1146 (1990).
34. A. Sulkowska, *J. Mol. Struct.*, **614**, 227 (2002).
35. Y. J. Hu, Y. Liu, X. S. Shen, X. Y. Fang and S. S. Qu, *J. Mol. Struct.*, **738**, 143 (2005).
36. Y. J. Hu, Y. Liu and L. X. Zhang, *J. Mol. Struct.*, **750**, 174 (2005).
37. A. Papadopoulou, R. J. Green and R. A. Frazier, *J. Agric. Food Chem.*, **53**, 158 (2005).
38. J. Thipperudrappa, D. S. Biradar, M. T. Lagare, S. M. Hanagodimath, S. R. Inamdar and J. S. Kadadevaramath, *J. Photochem. Photobiol. A*, **177**, 89 (2006).
39. J. B. Xiao, J. W. Chen, H. Cao, F. L. Ren, C. S. Yang and Y. Chen, *J. Photochem. Photobiol. A*, **191**, 222 (2007).
40. J. Xiao, X. Chen, L. Zhang, S. G. Talbot, G. C. Li and M. Xu, *J. Agric. Food Chem.*, **56**, 910 (2008).

41. J. B. Xiao, M. Suzuki, X. Y. Jiang, X. Q. Chen, K. Yamamoto and M. Xu, *J. Agric. Food Chem.*, **56**, 2350 (2008).
42. B. Valeur, *Molecular Fluorescence: Principles and Applications*, Wiley (2001).
43. W. K. S., H. M. H. and D. C., *Biochemistry*, **32**, 389 (1993).